J Indian Acad Wood Sci
https://doi.org/10.1007/s13196-017-0202-1

ORIGINAL ARTICLE

Sensitivity of acoustic tools to variation in equilibrium moisture content of small clear samples of loblolly pine (*Pinus taeda*)

Charles Essien[1] · Brian K. Via[1] · Thomas Gallagher[2] · Timothy Mcdonald[3] · Lori Eckhardt[2]

Received: 25 August 2017 / Accepted: 16 November 2017

Abstract There are several types of acoustic tools commercially available for wood characterization, but they are generally classified into resonance and time-of-flight (ToF) tools. This classification is based upon the mode of velocity estimation for wood. In this study, we explored how the equilibrium moisture content of small clear wood samples (2.5 cm × 2.5 cm × 41 cm) affect the predictive capabilities of two types of acoustic tools namely a microsecond timer (ToF) and a resonance log grader (resonance). The results indicated the acoustic velocity is sensitive to equilibrium moisture content of loblolly pine, and sensitivity to EMC is similar for both type of tools. The acoustic velocity decreased by 32.9 and 28.8 m/s for ToF and the resonance acoustic tools respectively for a unit increase in EMC below fiber saturation point (FSP); 5.4 and 6.1 m/s respectively for a unit increase in EMC above FSP although the slope was statistically equivalent to zero. Also, the static MOE of the green samples was overestimated by 16% by both resonance and ToF tools with oven-dried density, while it was 72% when estimated with density at test. The insignificant slope coupled with better accuracy in MOE supports the hypothesis that the cell wall controls the acoustic velocity while the water in the lumen of the cell wall is insignificant. These results bring into question the standard use of green density to estimate acoustic MOE of live trees and oven dry density is instead recommended.

Keywords Fiber saturation point · Acoustic velocity · Static modulus of elasticity · Time-of-flight

Introduction

Mechanical properties including modulus of elasticity (MOE) and modulus of rupture (MOR) of wood from different tree species have been extensively studied over the years (Bodig and Jayne 1982; FPL 2010). They reported that, generally, MOE and MOR decrease with increasing moisture till the fiber saturation point (FSP) is attained, above which insignificant difference occur. For most timber species, the FSP occurs between 20 and 35% moisture content, hence one does not expect MOE to vary significantly above this moisture range. Similarly, the volume of wood changes (shrink or swell) in response to alterations in moisture content (MC) below the FSP but it remains constant above the FSP. This is because above the FSP, the free water which occupies the cell lumen does not affect the structural matrix of the wood constituents hence the load bearing properties (MOE and MOR) are unaffected. Therefore, MOE and MOR above the FSP are generally reported as the green condition or state (FPL 2010). On the other hand, wood density increases with increasing moisture both above and below FSP, hence the density attains the maximum value when the cell lumen is fully filled with free water. This is because the free water adds to the weight of the wood but the volume remains constant. Similarly, the basic density (which is the ratio of oven dried weight to fully saturated volume of the wood) is the possible minimum density value a wood can attains.

✉ Charles Essien
cze0017@auburn.edu

[1] Forest Products Development Center, SFWS, Auburn University, 520 Devall Drive, Auburn, AL 36849, USA

[2] School of Forestry and Wildlife Sciences, Auburn University, 602 Duncan Drive, Auburn, AL 36849, USA

[3] Biosystems Engineering Department, Auburn University, Auburn, AL 36849, USA

Published online: 24 November 2017

Consequently, one has to state the condition of the wood under which the density was determined (FPL 2010). Generally, wood is utilized in the dry condition below the FSP hence most of the mechanical and technological properties are reported in either dry usually 12% MC or green or both. The use of acoustic techniques as a nondestructive MOE characterization tool for live trees, freshly cut logs, and other wood products requires density—(velocity^2 * density). The type of density to use continues to be one of the major challenges confronting the practitioners and researchers due the complex and confounding effect of MC on both density and velocity.

Wood is a dispersive material indicating that wave propagated through it changes frequency with passage (Beall 2002). Generally, wood acoustic quantification involved the transmission of high energy sound waves through the tissue to ascertain internal stiffness. The acoustic velocity of wood is different with respect to the direction of propagation. It is about five times higher in longitudinal direction as compared to that in the transverse direction. Similarly, it is estimated to be about 50% higher in the radial when compared to the tangential direction (Harris and Andrews 1999; Beall 2002; Chauhan and Walker 2006; Hasegawa et al. 2011). The acoustic velocity has been found to decrease with increasing equilibrium moisture content until the fiber saturation point, above which changes in moisture insignificantly affect velocity (Olivito 1996; Chan et al. 2011; Gao et al. 2012).

Above the fiber saturation point, for example, moisture content positively and significantly affects the density of wood (FPL 2010), but it does not significantly influence velocity (Gao et al. 2012). This relationship is further compounded by the effect of temperature and relative humidity. There are several studies undertaken to understand the effect of moisture content and temperature on acoustic velocity in order to determine correction factors to adjust the velocity to the desired moisture and/or temperature (Sandoz 1991; Kang and Booker 2002; Chan et al. 2011). But less is understood about how different acoustic based techniques differ in their response to moisture variation for the same test materials. This is important because various types of acoustic tools are designed for different wood products. For example, time-of-flight (TOF) acoustic tools are designed primarily to estimate the velocity of live trees whose moisture content rarely drop below FSP. However, resonance tools are designed for logs and wood products whose moisture can be above or below FSP. Thus a head to head comparison between tools across the entire moisture range is needed.

The longitudinal velocity decreased dramatically with increasing equilibrium moisture content (EMC) up to the FSP for both the resonance based tool (Kang and Booker 2002; Goncalves and Leme 2008; Chan et al. 2011; Yang et al. 2015) and time-of-flight based tool (Wang 2008). However, the rate of change in velocity is much lower when EMC was above FSP (Chan et al. 2011; Yang et al. 2015). Chan et al. (2011) found that acoustic velocity decreased by 32 m/s for a unit increase in moisture content below the fiber saturation point while the change ranged between 6 and 10 m/s for moisture above fiber saturation point for the resonance based tools. Since the different type of acoustic tools estimates velocity with different algorithms, it would be useful to understand the behavior of the velocity—EMC relationship for both the resonance and TOF acoustic tools. We hypothesized that for the same specimen and moisture content, the resonance tools will be more sensitive to variations in moisture content below FSP as compared to the TOF tools because resonance tools are designed for products having moisture content both above and below FSP while the TOF tools are generally meant for trees with moisture above the FSP. It should be noted that, though the TOF tools are designed for trees, they can be used on logs and other products as well. Therefore the main objectives of this study were to:

1. To examine the level of relationships among the static MOE and the dynamic MOEs predicted using both the green and oven dry densities.
2. To explore the sensitivity of acoustic tools to variation in EMC below and above the fiber saturation point of loblolly pine.

Materials and methods

Materials

The materials for this study were obtained from a plantation of genetically improved loblolly pine (*P. taeda*) families established in the year 2000. The trees were sampled by the Southern Forest Health Cooperative at Auburn University when they were 14 years old (Essien et al. 2017a, b). The plantation was located in Nassau County Florida near Yulee (latitude 30°63′N and longitude 81°57′W). The soil was poorly drained and formed from a thick bed of alkaline loamy and clayey marine sediments terraces with a slope less than 1%. The mean long-term temperature and precipitation from 1981 to 2010 are 21 °C and 1350 mm respectively (NOAA 2016). It should be noted that this study was not aimed at quantifying the variations within the genetic families but instead materials from different families were selected to ensure that the results were reflective of a wood mix that is common in today's market.

The trees were bucked into small billets and were further converted into small clear samples with dimensions of

25 mm × 25 mm × 410 mm in the radial, tangential and longitudinal directions respectively. The mean moisture content (MC) of all the samples was 62%. Forty-five (45) samples were used for the conditioning study and additional fifteen samples were used for static modulus of elasticity (MOE) and modulus of rupture (MOR) determination following ASTM D143.

Acoustic measurement

Two acoustic tools namely FAKOPP Microsecond Timer (TOF) and FAKOPP Resonance Log Grader (R) (Fakopp Enterprise, Agfalva, Hungary) were used to determine the acoustic velocity of each sample. The FAKOPP Microsecond Timer relies on measuring the time it takes for the generated stress waves to travel a known distance between two probes. The tool is equipped with a pair of piezo sensors (SD 20/60) by the manufacturer. Basically, the sensors (the transmitter and the receiver probes) were positioned on the same side of the samples. Both probes were positioned 45° to the sample plane and the stress wave was generated by striking the transmitter probe with a steel hammer at a steady force (Mora et al. 2009). The generated wave was detected by the receiver and the time lapse for the sound wave to travel the distance between the probes was recorded by the data logger (Fig. 1). The data logger displays the time and velocity determined using Eq. 1.

$$V_{TOF} = D/t \quad (1)$$

where V_{TOF} is the velocity estimated by the TOF (FAKOPP Microsecond Timer) tool, D is the distance between the probes, t is the time for the sound wave to travel the distance between the probes.

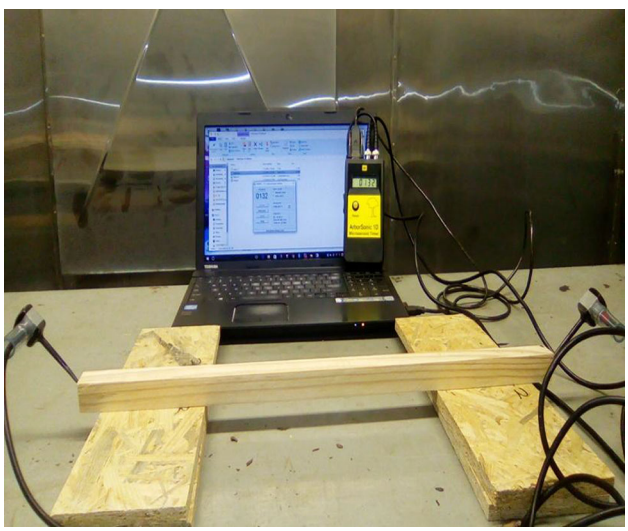

Fig. 1 Setup for the estimation of the acoustic velocity using Microsecond Time

Fig. 2 Setup for the estimation of acoustic velocity using resonance log grader

The FAKOPP Resonance Log Grader (R) tool determined the velocity using the resonance principle. The sample length is entered and the tool held firmly at the end of the sample. The wave is generated by striking the end of the sample with a hammer, the microphone picks up the acoustic wave signal as it resonates back and forth along the entire length of the sample at a rapid rate of hundreds of passes per second (Fig. 2), and display the velocity according to Eq. 4 (Wang et al. 2007).

$$V_R = 2f_1L \quad (2)$$

where V_R is the velocity estimated by the resonance tool, f_1 is the natural fundamental frequency mode (Hz), L is the length (m) of the sample.

All the forty-five small clear samples were weighed to the nearest 0.001 g and dimensions measured using digital calipers to the nearest 0.025 mm. The samples were subjected to a drying process in an airtight conditioning chamber set at a temperature of 22.7 °C and 55% relative humidity. Due to the smaller dimensions of the samples used in this study, rubber band were used to fasten to stakes to a fixed wooden platform (Figs. 1, 2) to prevent sample displacement during the acoustic testing. The samples were acoustically tested after 12 h exposure period using both FAKOPP Resonance Log Grader and FAKOPP Microsecond Timer acoustic tools. Six readings per sample were taken for each tool at any testing schedule in the conditioning chamber. Acoustic readings, dimensions and weight of the samples were then taken twice daily for the first week, after which readings were taken once a week. It should be note that, the same set of samples were repeatedly used at each measurement cycle (Fig. 3). This repetitive process continued until the samples attained constant

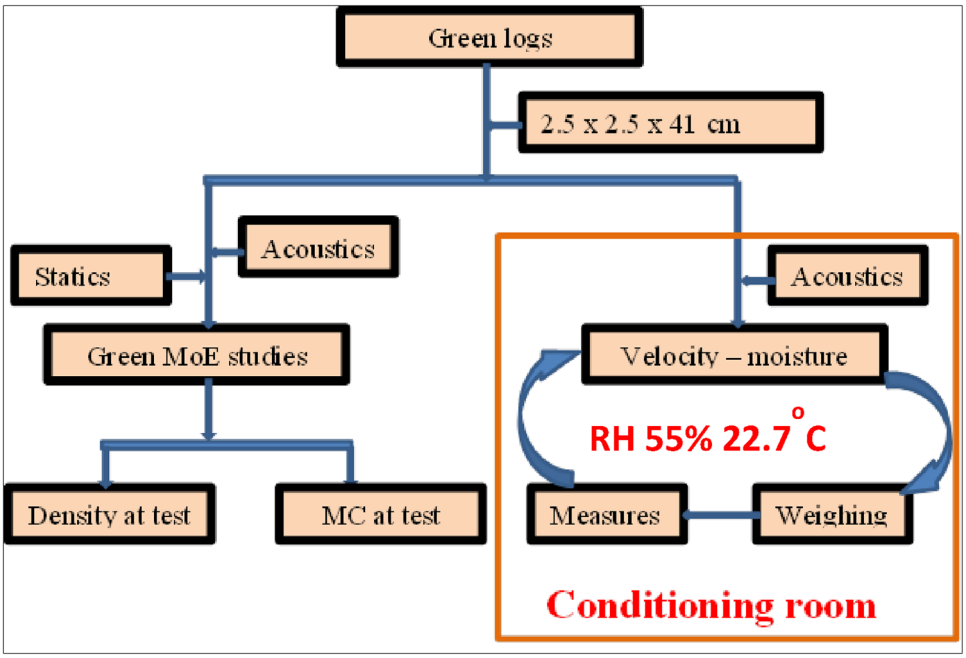

Fig. 3 Flow chart of the experimental set-up

weight in the chamber. The samples were then transferred to an electronic thermostatic oven set to 105 °C. The 105 °C was meant to oven dry the samples to zero percent moisture content. The EMC and density (GD) of the samples at each stage of the conditioning process were determined using Eqs. 3 and 4 respectively (FPL 2010). The oven dried density (OD) was determined as the ratio of the oven dried weight to the oven dried volume measured using digital calipers.

$$\mathrm{EMC} = (\mathrm{M_i} - \mathrm{M_o}/\mathrm{M_o}) * 100 \quad (3)$$

where $\mathrm{M_i}$ is the initial weight and $\mathrm{M_o}$ is the oven dried weight

$$\mathrm{GD} = \mathrm{weight}/\mathrm{volume} \quad (4)$$

where GD is the density at test, weight and volume are the measurement taken at each measurement period in an air-tight conditioning chamber.

Static MOE and MOR determination

Static MOE and modulus of rupture (MOR) were determined using the fifteen green small clear specimens measuring 2.5 × 2.5 × 41 cm (radial × tangential × longitudinal). Green samples were used because the moisture in healthy tree is above the FSP (green condition). The static bending tests were performed following the protocols of ASTM D143 (ASTM D143 2007). The load was applied on the tangential-longitudinal face in a three-point configuration using a Z010 Zwick Roell Testing System (Zwick Roell, Kennesaw, GA, USA) at a loading rate of 1.3 mm/min. The linear portion of the load–deflection curve was used to determine MOE, while MOR was calculated using maximum bending moment at the maximum load borne by the specimen. The moisture content and density at test were determined following the protocols described in ASTM D143. The density was determined by measuring the dimensions of the samples with calipers to the nearest 0.025 mm and the weight to the nearest 0.001 g.

The dynamic MOE of the samples were also determined using Eqs. 5 and 6 for the resonance and the time-of-flight tools respectively.

$$\mathrm{DMOE_R} = (\mathrm{V_R})^2\rho \quad (5)$$

$$\mathrm{DMOE_{TOF}} = (\mathrm{V_{TOF}})^2\rho \quad (6)$$

where $\mathrm{DMOE_R}$ is the dynamic MOE estimated by the Resonance Log Grader tool, $\mathrm{V_R}$ is the velocity determined by Resonance Log Grade, ρ is the density (kg/m^3), $\mathrm{DMOE_{TOF}}$ is the dynamic MOE estimated by the FAKOPP Microsecond Timer, $\mathrm{V_{TOF}}$ is the velocity estimated by the FAKOPP Microsecond Timer tool. The addition of GD and OD to the dynamic MOE—($\mathrm{DMOE_{ROD}}$, $\mathrm{DMOE_{RGD}}$, $\mathrm{DMOE_{TOFOD}}$, and $\mathrm{DMOE_{TOFGD}}$) indicated the type of density used in the computation. GD and OD indicated density at test and oven-dried density respectively was used for the computation of their associated dynamic MOE.

Data analysis

The data was analyzed using proc mixed in SAS 9.4 (SAS 2014). The model was fitted for the tool, EMC below and

above fiber saturation points (emc1 and emc2 respectively) and the two-way interaction terms (Eq. 7)

$$Y_{ijk} = \beta_0 + \beta_1 \text{tool} + \beta_2 \text{emc1} + \beta_3 \text{emc2} + \beta_4 \text{tool} * \text{emc1} + \beta_5 \text{tool} * \text{emc2} + \varepsilon_{ijk} \quad (7)$$

where Y_{ijk} is the velocity of ith sample, jth EMC, and kth tool, β_0, β_1, β_2, β_3, β_4, β_5 are the intercept, mean change in velocity due to tool, mean change in velocity due to EMC1 below fiber saturation, mean change in velocity due to EMC2 above fiber saturation, interaction term for the tool and EMC below and above fiber saturation points (FSP) respectively. These parameters were tested whether they are significantly different from zero.

The analysis of variance of the fitted model in Eq. 7, indicated that EMC1 and tools have significant effect on velocity while there are no significant interaction term and EMC2. Hence simple linear regression models were fitted for each tool at EMC below and above FSP (emc1 and emc2) Eq. 8.

$$\text{Yi} = \text{a} + b * \text{EMC} + \varepsilon_i \quad (8)$$

where ***Y*** is the mean velocity, ***a*** is the intercept and ***b*** is the mean rate of change in EMC below and above FSPs for each tool.

Results and discussions

Density

The density result is presented in Fig. 4. There is a general decrease in mean density as equilibrium moisture content in the samples decreased (Fig. 4). This results is in agreement with several previous reports (FPL 2010; Chan et al. 2011). Chan et al. (2011) reported linear increase in density with moisture content when they studied radiata pine boards. The fiber saturation point for loblolly pine has been reported to occur within 20–30% moisture content (FPL 2010). Based on our density and acoustic measurements, the FSP appeared to be around 29%, especially given the sharp drop in density at 29% (Fig. 4). The density of wood is a function of the wood material and the amount of water contained therein. When wood interacts with water, both the weight and dimensions of the wood change until the fiber saturation point is attained after which additional water absorption increase the weight of the wood with no alteration to the dimension. Hence, above the fiber saturation point, the density of wood is highly influenced by the weight of the moisture hence reduction in moisture leads to a significant decrease in density as shown in Fig. 4. Below the fiber saturation point, however, reduction in moisture caused both shrinkage in the volume and a reduction in weight resulting in a slight decrease in density (Fig. 4) (FPL 2010). Since the volume of the wood decrease but the weight of the wood material remains relatively constant at certain point below the fiber saturation point (oven dried weight), the density tends to increase as desorption progresses well below the saturation point.

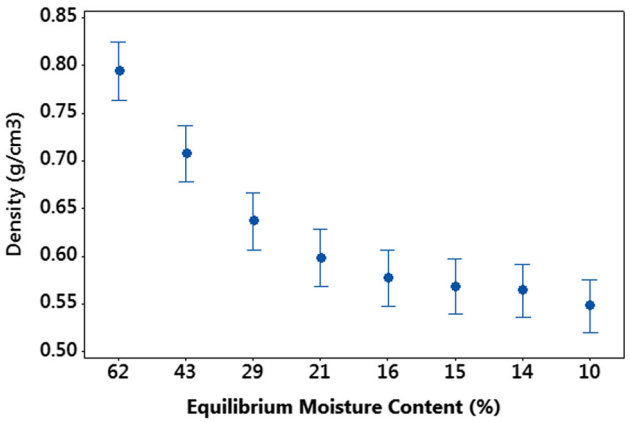

Fig. 4 Relationship between mean density and EMC

Static and dynamic properties of the green small clear samples

The results of the green static MOR, static, and dynamic MOE are presented in Table 1 and Figs. 5, 6, 7 and 8. The mean and coefficient of variation (COV) of the green static MOE and MOR are 7.3 GPa and 29% and 51.6 MPa and 25% respectively. The green MOE reported in this study is 25% lower than as stated in FPL (2010), but 87% higher than as reported by Moya et al. (2013) when they studied 15-year-old loblolly pine grown in the subtropical part of Uruguay. Similarly, the MOR of the present study is 70% higher than as reported by Moya et al. (2013). The differences in the strength and stiffness values are due to several factors such as edaphic, environmental, and the genetic stock of the planting materials. Moya et al. (2013) stated that the mean diameter at breast height of the trees was 30 cm which is 90% larger than ours of similar age. Generally, the slower growing trees in this study produced a higher proportion of latewood comprising of a thick cell wall, lower MFA, longer fibers, high MOE, and density as compared to the higher proportions of earlywood produced by fast growing trees. Therefore, even though loblolly pine between 11 and 15-year old is considered juvenile wood (Bendtsen and Senft 1986; Clark et al. 2006), the growth rate and the genetic sources of the planting material can improve the mechanical properties significantly. For this study, the growth rate was slow due to poor site nutrient conditions while the elite families were present. It is likely that the combination of these two factors help to explain the unusually high mechanical properties as such a young

Table 1 Descriptive statistics of the green static MOE and MOR, dynamic MOE estimated by resonance log grader ($DMOE_R$), Microsecond Timer ($DMOE_{ToF}$)

	Static MOE (GPa)	Static MOR (MPa)	$DMOE_{ROD}$ (GPa)	$DMOE_{ToFOD}$ (GPa)	$DMOE_{RGD}$ (GPa)	$DMOE_{ToFGD}$ (GPa)	Green density (kg/m^3)
Mean	7.35	51.55	8.55	8.73	12.67	12.85	901.79
SD	2.11	12.68	2.06	2.82	2.78	3.75	75.46
CoV	28.68	24.60	24.09	32.30	21.96	29.20	8.37
Min	3.46	30.6	5.52	2.75	9.11	4.58	800.2
Max	10.20	75.0	11.94	12.89	17.66	17.71	1026.1

$DMOE_{ROD}$ and $DMOE_{RGD}$ are dynamic MOEs estimated by resonance based tool with oven-dried density and density at test respectively

$DMOE_{ToFOD}$ and $DMOE_{ToFGD}$ are dynamic MOEs estimated by time-of-flight based tool with oven-dried density and density at test respectively

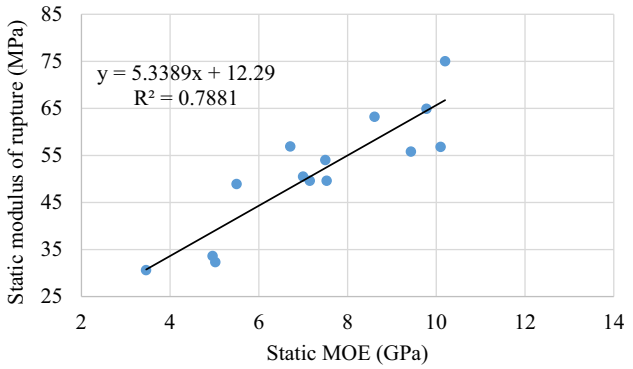

Fig. 5 Relationship between the green static MOR and static MOE for 15 small clear samples

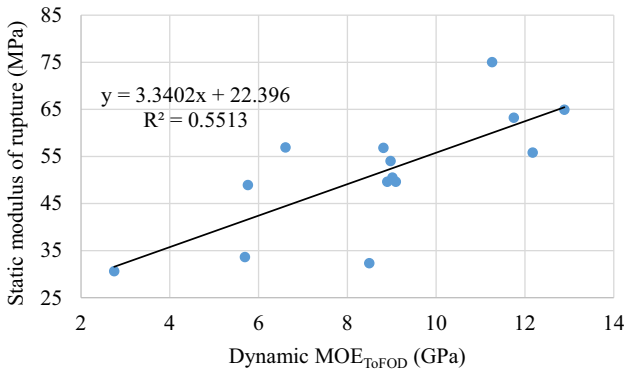

Fig. 6 Relationship between the green static MOR and dynamic MOE estimated by time-of-flight based tool with oven-dried density ($DMOE_{TOFOD}$)

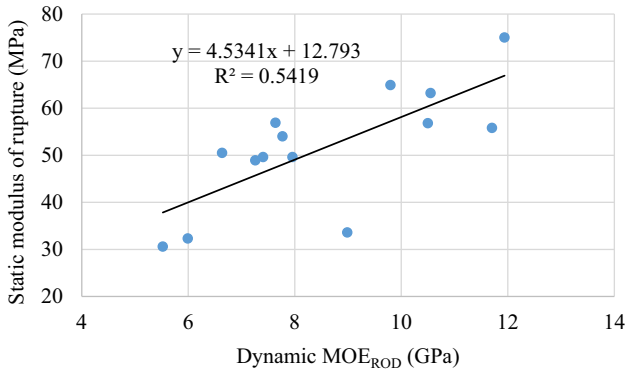

Fig. 7 Relationship between the green static MOR and dynamic MOE estimated by Resonance based tool with oven-dried density ($DMOE_{ROD}$)

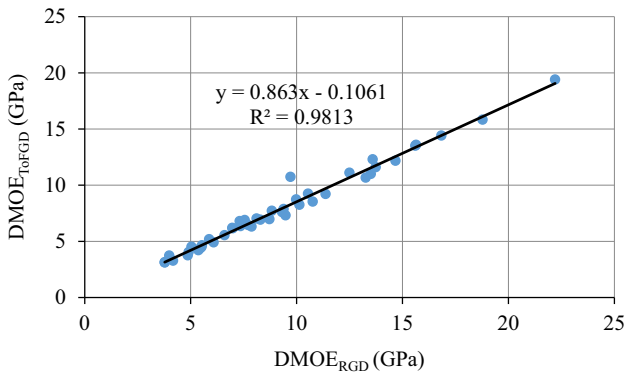

Fig. 8 Relationship between the dynamic MOE estimated by Microsecond Timer ($DMOE_{TOFGD}$) and Resonance Log Grader ($DMOE_{RGD}$) for the 45 small clear samples

age. Others have seen similar strength values for loblolly pine Moya et al. (2013).

There is a strong positive linear relationship between the green static MOE versus $DMOE_{TOFOD}$ and $DMOE_{ROD}$ with adjusted coefficient of determination (R^2_{adj}) of 72 and 68% respectively (Table 2). Similarly, the relationship between static MOE versus $DMOE_{TOFGD}$ and $DMOE_{RGD}$ yielded R^2_{adj} values of 71 and 56% respectively. However, it is worth noting that though the slopes of the regression between the static MOE versus MOE_{TOFOD}, MOE_{ROD}, MOE_{TOFGD}, and MOE_{RGD} were 0.64, 0.86, 0.48, and 0.58 respectively and they were statistically different (Table 2). The overlapping nature of the 95% confidence intervals

Table 2 Linear models ($y = a + bx$) of the relationships between the green static MOR, MOE (MOE_{st}), and dynamic MOE estimated by resonance log grader ($DMOE_R$), Microsecond Timer ($DMOE_{ToF}$) for 15 small clear samples

y	*x*	95% CL of *a*	95% CL of *b*	R^2_{adj}
MOR	MOE_{st}	12.29 (− 0.99, 25.59)	5.3 (3.6, 7.1)	77.04
	MOE_{ROD}	12.80 (− 10.2, 35.80)	4.5 (1.9, 7.2)	50.37
	MOE_{ToFOD}	22.4 (5.07, 39.72)	3.3 (1.4, 5.2)	51.39
	MOE_{RGD}	13.4 (− 14.5, 41.3)	3.0 (0.86, 5.2)	38.86
	MOE_{ToFGD}	20.01 (0.5, 39.53)	2.5 (1.0, 3.9)	48.78
MOE_{st}	MOE_{ROD}	25 (− 3067, 3117)	0.86 (0.51, 1.21)	67.58
	MOE_{ToFOD}	1745 (− 457, 3947)	0.64 (0.40, 0.88)	71.60
	MOE_{RGD}	− 37 (− 3982, 3908)	0.58 (0.28, 0.89)	55.80
	MOE_{ToFGD}	1169 (− 1268, 3606)	0.48 (0.30, 0.66)	71.10

$DMOE_{ROD}$ and $DMOE_{RGD}$ are dynamic MOEs estimated by resonance based tool with oven-dried density and density at test respectively

$DMOE_{ToFOD}$ and $DMOE_{ToFGD}$ are dynamic MOEs estimated by time-of-flight based tool with oven-dried density and density at test respectively

and the similitude of the R^2_{adj} suggested the dynamic MOEs estimated with both oven-dried (OD) density and density at test (GD) provides a reliable relationship with the static MOE. However, when the oven-dried density was used for Eqs. 5 and 6, the dynamic MOE was overestimated by 16% when compared to the static MOE. The density at test (GD) based dynamic MOE overestimated the static MOE on average by 72%. This suggests that though dynamic MOEs estimated with both densities provide similar strength of relationships with the static MOE, density at test (GD) based dynamic MOE significantly overestimate the static MOE. Wang et al. (2004) reported the slopes and the R^2 of the relationships between the green log static MOE and log dynamic MOE estimated by TOF for Red pine, Jack pine, Douglas fir, and Ponderosa pine to be 1.47, 0.79, 0.33, and 0.73, and 75, 60, 7, and 55% respectively. The slopes and the R^2 reported in the present study falls within the range reported by Wang et al. (2004) even though the dimensions of the studied sample differs between the two studies. It should be noted that all of the measurements in the present study were taken from the same small clear green samples contrary to what is usually reported in the literature where dynamic MOE of trees or logs is regressed against air dried small clear samples (Raymond et al. 2008; Mora et al. 2009; Yin et al. 2011) or both static and dynamic MOEs determined on air dry small clear samples (Chauhan and Sethy 2016). To the best of the authors' knowledge, there is no reported study using the green clear samples for both the static and the dynamic MOE determination. The semblance of the slopes and the R^2 in both the present and Wang et al. (2004) studies despite difference in sample dimension suggests that the drivers of the relationship between the static and dynamic MOEs are inherent in the wood independent of the dimensions of the wood material. Essien et al. (2017a, b) attribute the acoustic signal to be sensitive to the same suite of fiber morphology and chemistry as a real stick of wood which is important if acoustics is to be used for determination of stiffness in juvenile or younger wood. This is because Via et al. (2009) found MFA and lignin to be more relevant to stiffness in younger tissue while density and cellulose are more important for older growth material.

Similarly, there is a positive linear relationship between MOR vs static MOE, $DMOE_{TOFOD}$, $DMOE_{ROD}$, $DMOE_{TOFGD}$, and $DMOE_{RGD}$ with slopes 5.3, 3.3, 4.5, 2.5, and 3.0; and R^2_{adj} of 77, 51, 50, 49, and 39% respectively (Table 2). Butler et al. (2016) found a significant positive relationship between air-dried small clear loblolly pine sample MOR and MOE with slopes between 5.76–6.73, and 40–56% for R^2. Additionally, Moya et al. (2013) reported strong linear relationship between MOR and MOE of small clear green 25-year-old loblolly pine with R^2 of 77%. Ilic (2001a, b) reported $DMOE_R$ explained 69% variation in the static MOE of air dried small clear alpine ash samples. This moderate linear relationship between the static MOR and dynamic MOEs reported in the present study support the proposal that the acoustic tools can be used to characterize wood samples into MOR classes. Via et al. (2009) found that lignin and hemicelluloses become very important loading bearing component in the plastic deformation phase of the typical stress to strain curve of wood during bending while cellulose dominates the elastic phase of the curve. Hence demonstrating the significant effect of hemicelluloses on MOR. Essien et al. (2017a, b) demonstrated that the cellulose is the major driver of sound signal at the polymeric level with hemicellulose being the second most important signal conductor. This switch in role of hemicellulose might be the major contributor to the high relationship between the MOR and static MOE as compared to that with the dynamic MOEs. This is a subtle

but important point because conventional acoustics are traditionally based on elastic mechanics and MOR has traditionally just been assumed to covary with MOE.

Effect of EMC on velocity and dynamic MOE

From Table 3, velocity generally increased with decreasing equilibrium moisture content. This result confirmed several studies conducted in this area (Ilic 2001a, b; Kang and Booker 2002; Goncalves and Leme 2008; Hasegawa et al. 2011; Yang et al. 2015). The inverse relationship between velocity and EMC may be due to the impedance which increases with increasing moisture content (Yang et al. 2015). This is because the moisture in the cells (below FSP) interacts with the waves resulting in an absorption, refraction, and reflection of the waves leading to attenuation in energy. Consequently affecting the damping behavior of sound. This process ultimately results in a decreased velocity of wave propagation in wood (Yang et al. 2015). Alternatively, the velocity of sound in free water is approximately 1500 m/s which is lower than that of dry wood which is about 4500 m/s. As the wood dries, the moisture decreases leaving behind the relatively higher sound conducting wood material as shown in Table 3.

There is a significant difference between the mean rate of change in velocity with EMC below and above the hygroscopic region of the samples (Table 4). The mean rate of change in velocity per unit change in EMC is 33.9 and 5.4 m/s for the below and above FSPs respectively for the TOF tool while they are 28.8 and 6.1 m/s respectively for the resonance ones (Table 4). Several reports have also shown sharp decrease in acoustic velocity with increasing moisture content below fiber saturation point (Yang et al. 2015; Chan et al. 2011). Chan et al. (2011) found 32 m/s decrease in velocity per unit increase in moisture content below FSP and 6 m/s decrease in velocity for moisture content above FSP when they used resonance-based acoustic tool. From Table 4, the change in velocity above the hygroscopic region is not significantly different from zero hence one can deduce that velocity is unaffected by free water present in the cell lumen. This suggests that the cell walls are the major signal conducting avenue in the wood material instead of the cell lumen hence the presence of free water in the lumen does not significantly affect the velocity. Therefore, for healthy standing (live) trees and fresh logs, one will not expect moisture to drop below the hygroscopic region hence changes in moisture content will not significantly affect velocity. Operationally, this observation is important on two fronts (a) one does not need to measure or control for moisture content in the field and perhaps most importantly, (b) any change in density due to changes in free water within the tree is just adding random and unnecessary error to the estimate of MOE (Eqs. 5, 6). Instead, only oven dry density can be used in Eqs. 5 and 6 to capture real trends or differences in mechanical properties between trees.

Table 3 Descriptive statistics of the effect of EMC on velocity estimated by resonance and ToF acoustic tools

EMC (%)	Resonance		ToF	
	Mean (km/s)	CoV (%)	Mean (km/s)	CoV (%)
62	3.08	21.81	3.34	21.30
43	3.10	21.30	3.40	21.81
29	3.30	20.21	3.52	20.21
21	3.45	19.19	3.65	19.19
16	3.54	18.55	3.76	18.55
15	3.62	18.80	3.87	18.80
14	3.68	18.65	4.04	12.29
10	3.85	17.95	4.15	11.94

EMC Equilibrium moisture content, *CoV* coefficient of variation

The effect of EMC on dynamic MOEs estimated with both tools are shown in Figs. 9 and 10. Generally, dynamic MOE increases with decreasing EMC below the fiber saturation point. This is due to confounding and complex relationships between moisture versus velocity, moisture versus density, and density versus velocity. Below the fiber saturation point, velocity becomes the main driver of the dynamic MOE (Eqs. 5, 6) since the bound water content which acts as a signal dispersant, absorbance or reflectance decreases and the density stabilizes (Fig. 4). The net effect of these factors caused an increase in DMOE for both tools with decreasing EMC (Figs. 9, 10). On average, $DMOE_R$ decreased by 0.53 GPa whereas $DMOE_{TOF}$ decreased by 0.61 GPa for EMC from 10 to 29%. Chan et al. (2011) reported 0.71 GPa decrease in $DMOE_R$ for EMC from 17 to 25% when they studied $8 \times 5.5 \times 105$ cm^3 radiata pine sapwood while Ilic (2001a, b) reported 0.81 GPa reduction in $DMOE_R$ for EMC from 16 to 30% when he studied $9.5 \times 4.5 \times 60$ cm^3 Eucalyptus heartwood. The difference in $DMOE_R$ reduction values may be due to the moisture range studied as well the type and dimensions of wood species used.

On the other hand, DMOE increased slightly with increasing EMC above the fiber saturation point thus from 43 to 62% (Fig. 9) (Gerhards 1975; Sobue 1993). $DMOE_R$ increase by 0.18 GPa whereas that of $DMOE_{TOF}$ is 0.2 GPa. This observation is due to the counterbalancing effect of density and velocity (Fig. 1, Table 3). The percentage increase in squared velocity from 29 to 62% were 11 and 15% for the resonance and TOF based tools respectively while percentage decrease in density for the same EMC range was 33%. This counterbalancing effect in the computation of the DMOE might be responsible for this phenomenon. However, this may be erroneous since one

Table 4 Fit statistics for the simple linear regression E [Y_{ijk}] = a + b * EMC predicting mean velocity for each acoustic tool for EMC below and above fiber saturation points

Tool	Microsecond Timer			Resonance log grader		
	a	b	R2	a	b	R2
EMC below fsp	4.436	− 0.0339	92.40	4.069	− 0.0288	89.10
	(4.201,4.671)	(− 0.047, − 0.021)		(3.738, 4.400)	(− 0.047, − 0.010)	
EMC above fsp	3.665	− 0.0054	84.6	3.437	− 0.0061	95.78
	(3.263,4.067)	(− 0.014, 0.003)		(2.871, 4.003)	(− 0.018, 0.006)	

a = intercept, b = slope, 95% confidence limit in bracket. The range including zero is not statistically different from zero

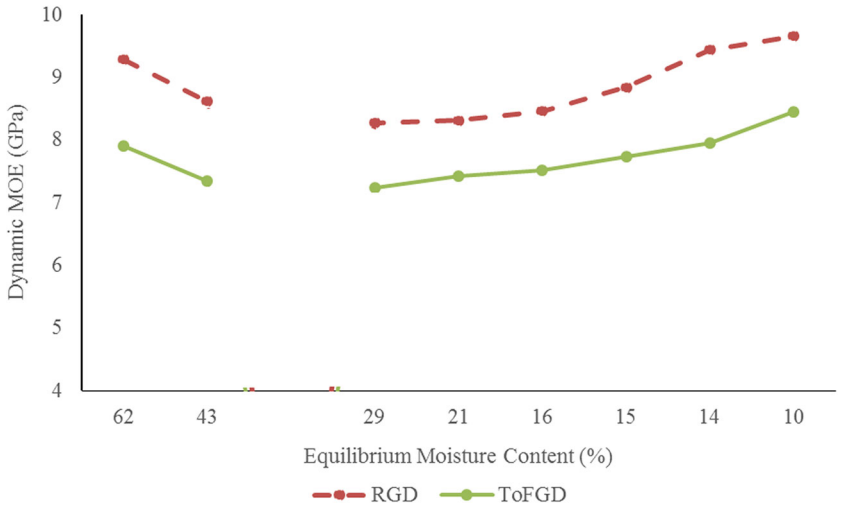

Fig. 9 Relationship between EMC and mean dynamic MOE estimated by the time-of-flight (TOFGD) and Resonance (RGD) tool with density at test (GD) (n = 45)

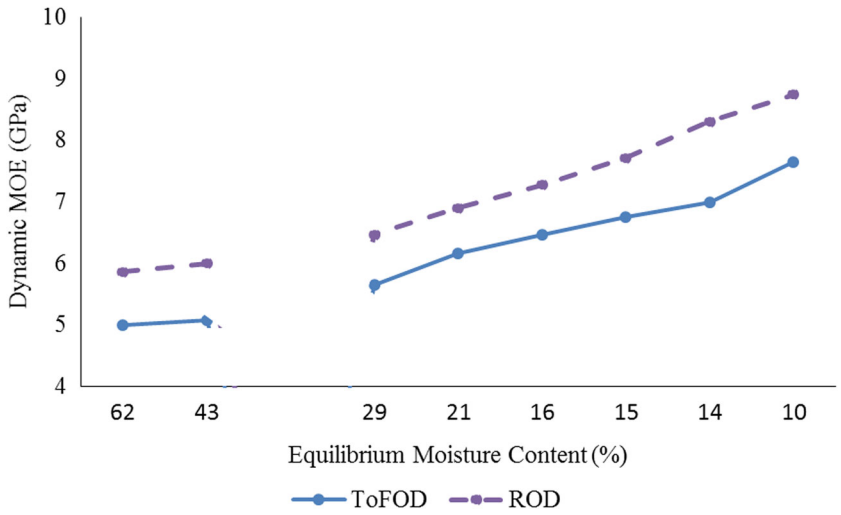

Fig. 10 Relationship between EMC and mean dynamic MOE estimated the time-of-flight (TOFGD) and Resonance (RGD) tool with oven-dried density (OD) (n = 45)

does not expect MOE to increase with moisture above the fiber saturation point FPL (2010). As indicated earlier, change in velocity with moisture above the fiber saturation is 5.8 and 6.1 m/s for the TOF and resonance tools respectively which is statistically not significantly different from zero, hence any ambiguity in the dynamic MOE (Fig. 9) may be due to the density used in the computation. Consequently, oven dried density was used to compute the dynamic MOE as shown in Fig. 10. It is clear that dynamic MOEs are relatively the same between 43 and 62% EMC but increase with decreasing EMC from 29 to 10%. This trend supports the established fact that above the FSP, mechanical properties do not vary significantly with moisture. Based upon this observation, dynamic MOE

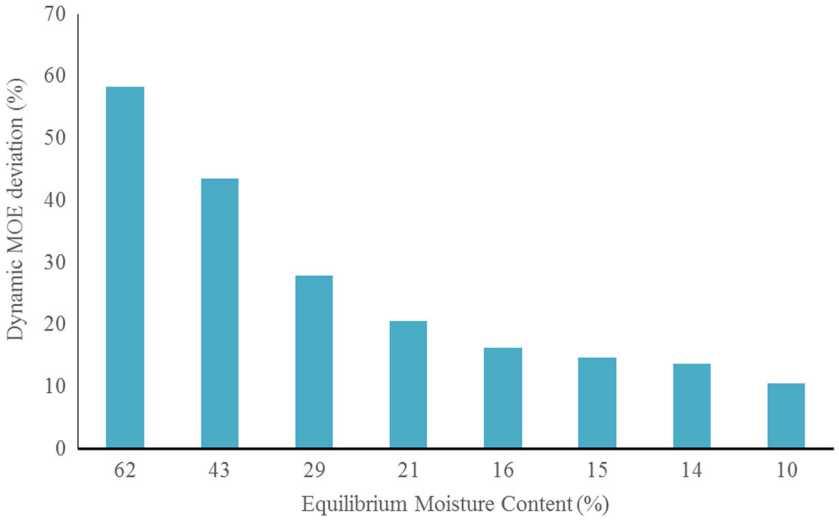

Fig. 11 Relationship between EMC and dynamic MOE deviation for the Resonance Log grader (RGD) tool (n = 45)

deviation was computed for the resonance tool according to Eq. 9 and results shown in Fig. 8.

$$\Delta MOE = 100 * \left(\frac{DMOE_{RGD} - DMOE_{ROD}}{DMOE_{ROD}} \right) \quad (9)$$

From Fig. 11, the percentage dynamic MOE deviation is a function of the EMC which decreases with decreasing EMC. It decreased from 27 to 9% below the fiber saturation point (29 to 10% EMC), but it was greater than 40% above the fiber saturation point. This suggests that using the density at test (GD) to estimate dynamic MOE of the standing tree or fresh log will overestimate it by at least by 40% as compared to using oven dried density.

Conclusion

The effect of equilibrium moisture content on acoustic velocity and dynamic MOE estimated by resonance and time-of-flight based acoustic tools were studied. The results indicated a strong positive relationship between the static MOE, MOR and dynamic MOEs estimated by both types of tools with the different densities. Also, the static MOE of the green samples exhibited similar strength of linear relationship with dynamic MOEs estimated with both the oven-dried density and density at test. However, for both acoustic tools, the static MOE was overestimated by about 16% when dynamic MOEs were estimated with oven-dried density (OD), but it was overestimated by about 72% when dynamic MOEs were determined with the density at test (GD). The results suggest that the OD density should be used when computing the dynamic MOE.

From this study, it has been demonstrated that using the density at test (green density) to predict the dynamic MOE of live trees and freshly harvest logs, with the moisture above the FSP, will be at least 40% higher than similar prediction using oven-dried density. Also, the study supports the idea that acoustic tools can be used to characterize wood into strength classes.

Furthermore, equilibrium moisture content of loblolly pine significantly affects velocity measured below and above the hygroscopic region. The results indicated the acoustic velocity decreased by 33.9 and 28.8 m/s for time-of-flight and the resonance tools respectively for unit increase in EMC below fiber saturation point. The change was lower for EMC above FSP—5.4 m/s for TOF and 6.1 m/s for resonance. The insignificant slope coupled with better accuracy in MOE supports the hypothesis that the cell wall controls the acoustic velocity while the water in the lumen of the cell wall is insignificant. These results bring into question the standard use of green density to estimate acoustic MOE and oven dry density is instead recommended. On average, $DMOE_R$ decreased by 0.53 GPa whereas $DMOE_{TOF}$ decreased by 0.61 GPa for EMC from 10 to 29%. These results suggest that the both tools are equally sensitive to variations in EMC below and above FSP.

References

ASTM Standard D 143-94 (2007) Standard test methods for small clear specimens of timber. ASTM International, West Conshohocken, Pa. Available at www.astm.org. Accessed 5 Jan 2014

Beall FC (2002) Overview of the use of ultrasonic technologies in research on wood properties. Wood Sci Technol 36:197–212

Bendtsen BA, Senft J (1986) Mechanical and anatomical properties in individual growth ring of plantation-grown cottonwood and loblolly pine. Wood Fiber Sci 18(1):23–38

Bodig J, Jayne BA (1982) Mechanics of wood and wood composites. Van Nostrand Reinhold Company Inc, NY, pp 584

Butler MA, Dahlen J, Antony F, Kane M, Eberhardt TL, Jin H, Myers KL, McTague JP (2016) The relationship between loblolly pine

small clear specimens and dimension lumber test in static bending. Wood Fiber Sci 48(2):81–95

Chan MJ, Walker CJ, Raymond CA (2011) Effect of moisture content and temperature on acoustic velocity and dynamic MOE of radiata pine sapwood boards. Wood Sci Technol 45:609–626. https://doi.org/10.1007/s00226-010-0350-6

Chauhan S, Sethy A (2016) Differences in dynamic modulus of elasticity determined by three vibration methods and their relationship with static modulus of elasticity. Maderas Ciencia y Technologta 18(2):373–382. https://doi.org/10.4067/S0718-221X2016005000034

Chauhan SS, Walker JCF (2006) Variations in acoustic velocity and density with age, and their interrelationships in radiate pine. For Ecol Manag 229(1–3):388–394. https://doi.org/10.1016/j.foreco.2006.04.019

Clark A, Daniels RF, Jordan L (2006) Juvenile/mature wood transition in loblolly pineas defined by annual ring specific gravity, proportion of larewood, and microfibril angle. Wood Fiber Sci 38(2):292–299

Essien C, Via BK, Gallagher T, McDonald T, Wang X, Eckhardt LG (2017a) Multivariate modeling of acousto-mechanical response of fourteen year old suppressed loblolly pine (*Pinus taeda*) to variation in wood chemistry, microfibril angle, and density. Wood Sci Technol 51:475–492. https://doi.org/10.1007/s00226-017-0894-9

Essien C, Via BK, Acquah G, Gallagher T, McDonald T, Eckhardt LG (2017b) Effect of genetic sources on anatomical, morphological, and mechanical properties of 14-year-old genetically improved loblolly pine families from two sites in the southern United States. J For Res **(in press)**

FPL (Forest Products Laboratory) (2010) Wood handbook—wood as an engineering material. General Technical Report FPL-GTR-190. Madison, WI: U.S. Department of Agriculture, Forest Service, Forest Products Laboratory, p 508

Gao S, Wang X, Wang L, Allison RB (2012) Effect of temperature on the acoustic evaluation of standing trees and logs: part 1—laboratory investigation. Wood Fiber Sci 44(3):286–297

Gerhards CC (1975) Stress wave speed and MOE of sweetgum ranging from 150 to 15 percent MC. For Prod J 25(4):51–57

Goncalves R, Leme OA (2008) The influence of moisture content on longitudinal, radial and tangential ultrasonic velocity for two Brazilian wood species. Wood Fiber Sci 40(4):580–586

Harris PD, Andrews MK (1999) Tools and acoustic techniques for measuring wood stiffness. In: Proceedings of the 3rd wood quality symposium: emerging technologies for evaluating wood quality for processing, Forest Industry Engineering Association, Rotorua, New Zealand

Hasegawa M, Takata M, Matsumura J, Oda K (2011) Effect of wood properties on within-tree variation in ultrasonic wave velocity in softwood. Ultrasonics 52:296–302

Ilic J (2001a) Variation of the dynamic elastic modulus and wave velocity in the fiber direction with other properties during the drying of *Eucalyptus regnans* F Muell. Wood Sci Technol 35:157–166

Ilic J (2001b) Relationship among the dynamic and static elastic properties of air-dry *Eucalyptus delegatensis* R. Baker. Holz als Roh 59:169–175

Kang H, Booker RE (2002) Variation of stress wave velocity with MC and temperature. Wood Sci Technol 36:41–54

Mora CR, Schimleck LR, Isik F, Mahon JM Jr, Clark A III, Daniels RF (2009) Relationship between acoustic variable and different measures of stiffness in standing *Pinus taeda* trees. Can J For Res 39(8):1421–1429. https://doi.org/10.1139/X09-062

Moya L, Laguarda ML, Cagno M, Cardoso A, Gatto F, O'Neill H (2013) Physical and mechanical properties of loblolly and slash pine wood from Uruguayan plantations. For Prod J 63(3/4):128–137. https://doi.org/10.13073/FPJ-D-13-00024

NOAA (National Oceanic and Atmospheric Administration) (2016) State, regional and national monthly precipitation: area weighted monthly normal, 1981–2015. Historical Climatography

Olivito RS (1996) Ultrasonic measurements in wood. Mater Eval 54:514–517

Raymond CA, Joe B, Anderson DW, Watt DJ (2008) Effect of thinning on relationships between three measures of wood stiffness in *Pinus radiata*: standing trees *vs*. short clear specimens. Can J For Res 38(11):2870–2879. https://doi.org/10.1139/X08-124

Sandoz JL (1991) Nondestructive evaluation of building timber by ultrasound. In: 8th international symposium on non-destructive testing of wood. Vancouver, Canada

Sobue N (1993) Simulation study on stress wave velocity in wood above fiber saturation point. Mokuzai Gakkaishi 39(3):271–276

Via BK, So CL, Shupe TF, Groom LH, Wikaira J (2009) Mechanical response of longleaf pine to variation in microfibril angle, chemistry associated wavelengths, density and radial position. Compos A 40(1):60–66

Wang X (2008) Effects of size and moisture content on stress wave E-rating of structural lumber. In: 10th world conference on timber engineering. Miyazaki, Japan

Wang X, Ross RJ, Brashaw BK, Punches J, Erickson JR, Forsman JW, Pellerin RE (2004) Diameter effect on stress-wave evaluation of modulus of elasticity of logs. Wood Fiber Sci 36(3):368–377

Wang X, Ross EJ, Carter P (2007) Acoustic evaluation of wood quality in standing tree. Part 1; acoustic wave behavior. Wood Fiber Sci 39(1):28–38

Yang H, Yu L, Wang L (2015) Effect of moisture content on the ultrasonic properties of wood. J For Res 26(3):753–757

Yin Y, Jiang X, Wang L, Bian M (2011) Predicting wood quality of green logs by resonance vibration and stress wave in plantation-grown Populus x euramericana. For Prod J 61(2):136–142